

Amino Acid Based Gallium-68 Chelators Capable of Radiolabeling at Neutral pH

Thomas W. Price,^{a,b} Juan Gallo,^c Vojtěch Kubiček,^d Zuzana Böhmová,^d Timothy J. Prior,^e John Greenman,^a Petr Hermann,^d and Graeme J. Stasiuk^{a,b}*

^a School of Life Sciences, Department of Biomedical Sciences, University of Hull, Cottingham Road, Hull, UK, HU6 7RX

^b Positron Emission Tomography Research Centre, University of Hull, Cottingham Road, Hull, UK, HU6 7RX

^c Advanced (magnetic) Theranostic Nanostructures Lab, International Iberian Nanotechnology Laboratory, Av. Mestre José Veiga s/n 4715-330 Braga, Portugal

^d Faculty of Science, Charles University, Hlavova 2030, 12840, Prague 2, Czech Republic

^e Chemistry, School of Mathematical and Physical Sciences, University of Hull, Cottingham Road, Hull, UK, HU6 7RX

*g.stasiuk@hull.ac.uk

Keywords: Gallium-68, Chelate, PET, Amino Acid, Radiolabelling

Abstract: Gallium-68 (^{68}Ga) has been the subject of increasing interest for its potential in the production of radiotracers for diagnosis of diseases. In this work we report the complexation of ^{68}Ga by the amino acid based tripodal chelate H_3Dpaa , and two bifunctional derivatives, $\text{H}_3\text{Dpaa.dab}$ and $\text{H}_4\text{Dpaa.ga}$, under a range of conditions with particular emphasis on the rapid complexation of ^{68}Ga at pH 7.4. 100 μM H_3Dpaa achieved a radiochemical yield of 95% at pH 7.4 in 5 minutes at 37 $^\circ\text{C}$. The bifunctional derivatives $\text{H}_4\text{Dpaa.ga}$ and $\text{H}_3\text{Dpaa.dab}$ achieved 94% and 84% radiochemical yields, respectively, under the same conditions. The resulting Ga(III) complexes show thermodynamic stabilities of $\log K_{\text{GaDpaa}} = 18.53$, $\log K_{\text{GaDpaa.dab}} = 22.08$, $\log K_{\text{GaDpaa.ga}} = 18.36$. Unfortunately, the resulting radiolabelled species do not present sufficient serum stability for *in vivo* application. Herein we show a flexible synthesis for bifunctional chelators based on amino acids that rapidly complex ^{68}Ga under physiological conditions.

Introduction

Positron emission tomography (PET) is a highly sensitive imaging technique that has been widely applied in cancer diagnosis through the use of [^{18}F]-fluorodeoxyglucose (FDG).¹ However, FDG is taken up in all areas of enhanced metabolism.¹ More specific, targeted, probes will provide improved diagnosis. Whilst incorporation of ^{18}F and ^{11}C into small organic molecules can provide a route to targeted probes, this route often requires multistep syntheses with harsh reaction conditions that are not compatible with many biomolecules.^{2, 3} More rapid assessment of new targeting motifs may be achievable by exploiting the modular system created by conjugation of targeting motifs to bifunctional chelates that complex radiometals such as ^{68}Ga , ^{64}Cu or ^{89}Zr .^{4, 5}

Of these positron emitting metal isotopes, ^{68}Ga is of particular interest.⁶⁹ The generator source of ^{68}Ga allows for local production at the site of use, opening the possibility of individual hospitals producing their own radiotracers instead of relying upon centralised production facilities. Comparisons can be drawn to the successful $^{99\text{m}}\text{Tc}$ single photon emission computed tomography (SPECT) isotope.¹⁰ The 68 minute half-life of ^{68}Ga is amenable to imaging with peptides and other molecules with relatively short blood circulation times in vivo.¹¹

Traditional macrocyclic chelators, including 1, 4, 7, 10-tetraazacyclododecane-1, 4, 7, 10-tetraacetic acid (DOTA), have been successfully applied to ^{68}Ga complexation.¹⁵¹⁷ Conjugated DOTA derivatives have been applied to imaging of neuroendocrine tumours – with [^{68}Ga]-DOTATATE being recently approved for use by the FDA. However, radiolabeling of DOTA with ^{68}Ga requires relatively aggressive conditions, a pH of 4 and heating to over 80 °C for efficient radiolabeling.^{15, 18} These conditions limit the range of targeting motifs that can be used with [^{68}Ga]-DOTA to acid and temperature stable species.

A range of chelators have been tested for their ^{68}Ga complexation abilities.^{4, 12-14} Recent trends in chelate design for ^{68}Ga have been to improve the radiolabeling procedure by reducing the temperature required for efficient complexation of ^{68}Ga and raising the pH at which this occurs.^{4, 12, 19, 20} This is a challenge due to the formation of kinetically inert gallium hydroxide species above pH 4.5.^{6, 10} Radiolabelling at pHs and temperatures close to physiological conditions is necessary to maintain the structure of peptides and aptamers. Furthermore, radiolabelling at neutral pH would reduce the formulation required after synthesis of the radiotracer, simplifying the tracer production procedure.

The smaller macrocycle, 1, 4, 7-triazacyclononane-1, 4, 7-triacetic acid (NOTA) has been applied to ^{68}Ga complexation, and radiolabelling proceeds efficiently at room temperature, although acidic conditions are still required.¹⁶ Novel, non-macrocyclic chelates THP²¹ and DATA²² have been shown to rapidly complex ^{68}Ga at higher pH values. While the conjugated DATA probe, DATA-TOC, has only been radiolabelled at pH 4-5,²³ THP conjugates, THP-RGD and THP-TATE, were radiolabelled at pH 5-6.5.^{24, 25} Despite this recent progress, rapid radiolabeling with ^{68}Ga at pH 7 has not yet been widely realised, with few bifunctional chelators capable of achieving rapid complexation at neutral pH reported (structures of these bifunctional chelators are shown in figure S1).²⁶⁻²⁸

Development of alternative chelates that can achieve this may allow for improved design of the imaging probe through different pharmacokinetic profiles/biodistributions.²⁹ While THP-TATE can be radiolabelled at pH 6.5, its lipophilic nature results in a significantly different biodistribution when compared to DOTA-TATE, with longer renal and liver uptake. Balancing improved radiolabeling properties with ideal imaging properties requires the development of new chelates to optimize both properties.²⁹

We report here the application of the chelate *N, N*-bis[(6-carboxypyridin-2-yl)methyl]glycine (H₃Dpaa) and two bifunctional derivatives, H₃Dpaa.dab and H₄Dpaa.ga (Figure 1) to ⁶⁸Ga complexation. H₃Dpaa is composed of two picolinic acid arms attached to a central glycine unit to produce a tripodal, hexadentate ligand. Picolinic acids have been demonstrated to be highly capable ⁶⁸Ga coordinating arms.³⁰ The aminebis(picolinic acid) motif has been applied to the complexation of a variety of metals with a number of different amines being used to form chelates with varying properties.^{31,42} The incorporation of a glycine residue into the chelate backbone provides both a carboxylic acid group that can bind strongly to Ga(III) due to a good hard acid/base match, and also a site which can be readily functionalised through application of other amino acids.^{31, 33} H₃Dpaa has previously been applied to complexation of lanthanide(III) ions such as gadolinium(III) ($\log K_{\text{GdDpaa}} = 10.6$)^{32, 33} and terbium(III) ($\log K_{\text{TbDpaa}} = 10.4$).³² H₃Dpaa has recently been applied to manganese(II) ($\log K_{\text{MnDpaa}} = 13.2$),³⁴ lanthanum(III) ($\log K_{\text{LaDpaa}} = 13.6$)³⁵ and gallium-67 ($\log K_{\text{GaDpaa}} = 18.7$)³⁵ complexation showing the versatility of this ligand for metal coordination. Herein we show a flexible synthesis for bifunctional chelators that rapidly complex ⁶⁸Ga under physiological conditions with a radiochemical yield of up to 95%. Unfortunately, the radiolabelled species [⁶⁸Ga][Ga(Dpaa)], [⁶⁸Ga][Ga(Dpaa.dab)] and [⁶⁸Ga][Ga(Dpaa.ga)] show poor stability in serum competition studies and are unsuitable for advancing to *in vivo* studies.

Results and Discussion

Synthesis and Characterisation

In this paper we report the application of *N, N*-bis[(6- carboxypyridin-2-yl)methyl]glycine (H₃Dpaa) and two bifunctional derivatives to ⁶⁸Ga complexation. The ligand H₃Dpaa was synthesized in two steps as described by Mazzanti *et al.*³² from ethyl 6-(chloromethyl)picolinate

and glycine ethyl ester hydrochloride followed by deprotection under acidic conditions. The bifunctional chelates, (*S*)-6,6'-(((3-amino-1-carboxypropyl)azanediyl)bis(methylene))dipicolinic acid (H₃Dpaa.dab) and *N,N*-bis((6-carboxypyridin-2-yl)methyl)-L-glutamic acid (H₄Dpaa.ga), were synthesised in a similar fashion from the relevant protected amino acid analogues, H-dab(Boc)-OMe hydrochloride³³ and diethyl glutamate hydrochloride as shown in Scheme 1. Et₄Dpaa.ga was obtained in a 72% yield as a yellow oil. Deprotection of this proligand via acid hydrolysis yielded H₄Dpaa.ga as an off white solid in an 82% yield. Crystals of H₄Dpaa.ga suitable for single crystal x-ray diffraction were obtained by precipitation from water. The obtained structure[†] (Figure S22) shows a distinct asymmetry caused by the chirality of the amino acid used. The molecule displays a configuration with one picoline ring on top of the other at a separation at little over 3 Å. This arrangement facilitates an intramolecular hydrogen bond between the glycine carboxylic acid and the pyridine (N2-H2...O6). The second picolinic acid is present with the nitrogen protonated and free carboxylate (N1-H1...O7ⁱ, where $i = x - \frac{1}{2}, \frac{1}{2} - y, z + \frac{1}{2}$). This arrangement facilitates an R₂²(8) embrace to the terminal carboxylic acid group of another molecule. In the solid there is an extensive hydrogen bond network.

Ga(III) complexes were synthesized by addition of GaCl₃ to an aqueous solution of the ligand. The resulting complexes precipitated out of solution and were collected.

Evidence for complexation can be seen through the distinct NMR resonances of the two protons in the CH₂ environment between the picolinate arms and the central amine. While these protons are equivalent ($\delta_{\text{H}_3\text{Dpaa}} = 3.92$, $\delta_{\text{H}_3\text{Dpaa.dab}} = 4.41$, $\delta_{\text{H}_4\text{Dpaa.ga}} = 4.40$) on the NMR time scale in the free ligands, in the Ga(III) complexes they are inequivalent ($\delta_{[\text{Ga}(\text{Dpaa})]} = 4.62$ and 4.48 , $\delta_{[\text{Ga}(\text{Dpaa.dab})]} = 4.56$ - 4.33 and 4.07 , $\delta_{[\text{Ga}(\text{Dpaa.ga})]} = 4.66$ and 4.33) and show a strong geminal coupling to one another ($^2J_{\text{HH}} = 16$ - 17 Hz).

Crystal structure of Ga(III) complexes

Single crystals of [Ga(Dpaa)] and [Ga(Dpaa.ga)] of a suitable quality for x-ray diffraction were obtained from acidic aqueous solutions. In each of the two structures: [‡], [§] Ga(III) is in a six coordinate environment, with five coordination sites occupied by the ligand and the final site by water. (Figure 2) The bonds from the Ga(III) atom to nitrogen atoms are rather longer than those to the oxygen atoms of the carboxylates (as shown in Table 1). This is a consequence of the strain in the ligand and may also reflect the preference of Ga(III) for the hard oxygen donors. The central amine atom (N2) in each structure is rather too distant from the Ga(III) to suggest a bond.

Each structure features a distorted octahedral coordination of the Ga(III) as a consequence of the geometry of the ligand. The greatest distortion is obvious in the plane of the picolinic acids (Tables 1 & 2). In each case the N1-Ga-N3 angle is greater than 133° and consequently the N-Ga-O angles are much smaller than the ideal 90° expected for undistorted octahedral geometry.

[Ga(Dpaa)] is relatively symmetric and there is a pseudo-mirror plane (through O3, N2, and O1w) present in the complex. The picolinate arms are close to planar; the angle subtended by the two mean planes of the picolines is 9.53(3)°. In contrast the glutamic acid backbone introduces a twist in [Ga(Dpaa.ga)] removing the pseudo-mirror plane and pushing the picolinate rings further out of the same plane such that the angle between their mean planes is 15.85(3)°. It is important to note that the pendant carboxylate arm of the glutamic acid is not involved in Ga(III) coordination. Full crystallographic data can be found in the supplementary information.

Potentiometry

Protonation constants of the studied compounds were determined by potentiometry (Table 3, distribution diagrams are shown in Figure S2). The determined protonation constants of H₃Dpaa are in very good agreement with those previously reported.^{32, 35} The first protonation constant ($pK_1 = 7.38$) is assigned to the central amine group. The two remaining constants are ascribed to protonation of the picolinate arms. The protonation constant of the pendant acetic acid group could not be determined due to its highly acidic nature.

The additional carboxylate group in H₄Dpaa.ga introduces an additional protonation constant in the weakly acidic region ($pK_2 = 4.67$). However, it does not alter significantly the protonation constants of the ligand core ($pK_1 = 7.33$) or the picolinate arms. The terminal amino group in H₃Dpaa.dab is protonated above pH 11 ($pK_1 = 11.35$). Presence of the additional protonated amino group significantly decreases basicity of the central amino group in the ligand core ($pK_2 = 5.39$).

Complexation of Ga(III), Cu(II) and Zn(II) ions by the three ligands was studied by potentiometry. These metal-ligand systems were chosen due to their importance for the potential application of these ligands to nuclear medicine. The results are summarized in Table 4.

The study of the Ga(III)-Dpaa system was not straightforward due to low solubility of the uncharged [Ga(Dpaa)] species. Therefore, UV-VIS titration was performed at significantly lower concentration (Figure S4). Nitrogen atoms of the ligands are weakly basic and this leads to complexation of metal ions even in strongly acidic solutions. As a consequence, some of the complexes were fully formed in the beginning of potentiometric titrations. Thus, Cu(II) and Zn(II) systems with H₄Dpaa.ga and H₃Dpaa.dab were also studied by UV-VIS spectrophotometry at pH 0–2 (Figure S6 and S8). Spectrophotometry was not employed in Ga(III) systems for these ligands

as stability constants could be determined from competition with hydroxide ions in the alkaline region (i.e. formation of $[\text{Ga}(\text{OH})_4]^-$).

The stability constants of $[\text{Ga}(\text{L})]$ species are similar for both H_3Dpaa and $\text{H}_4\text{Dpaa.ga}$. This indicates a negligible role of the distant carboxylate in complexation reactions of $\text{H}_4\text{Dpaa.ga}$ in agreement with crystallographic data. For $[\text{Ga}(\text{Dpaa.ga})]$, the first protonation constant ($[\text{M}(\text{L})] + \text{H} \leftrightarrow [\text{M}(\text{HL})]$, $\log K = 4.04$, Table S2) is comparable to that of free ligand, further supporting that the distant carboxylate group is not coordinated. In both systems, hydroxido species, $[\text{Ga}(\text{HO})(\text{Dpaa})]^-$ and $[\text{Ga}(\text{HO})(\text{Dpaa.ga})]^-$, are formed already in acidic region through a formal aqua ligand dissociation with corresponding pK_a values of 4.41 and 5.27, respectively.

This points to an unsaturated coordination sphere of the metal ion in these complexes in which some of the ligand donor groups remain uncoordinated. The unsaturated coordination sphere is corroborated by the crystal structures obtained in which this site is occupied by a bound water molecule. Complexes in which the coordination sphere of $\text{Ga}(\text{III})$ is not fully satisfied by a chelate with six coordinating atoms have been reported previously, with modelling suggesting either water or chloride bound in the vacant site.^{43, 44} Stability constants of the studied $\text{Ga}(\text{III})$ complexes are significantly higher than those reported for complexes of H_3Dpaa with lanthanide(III) ions ($\log K = 10.6$ and 10.4 for $[\text{Gd}(\text{Dpaa})]$ and $[\text{Tb}(\text{Dpaa})]$, respectively).³² This indicates that the ligands better suits “hard” and small metal ions such as $\text{Ga}(\text{III})$.

The stability constant for $[\text{Ga}(\text{Dpaa.dab})]$ complex ($\log K_{\text{GaL}} = 22.08$) is surprisingly much higher than those of the other two $\text{Ga}(\text{III})$ complexes. This is due to the different structure of the $[\text{GaL}]$ species. The $\text{Ga}(\text{III})$ ion in $[\text{Ga}(\text{Dpaa})]$ and $[\text{Ga}(\text{Dpaa.ga})]$ complexes is coordinated by the fully deprotonated ligand. Ligand $\text{H}_3\text{Dpaa.dab}$ contains the highly basic terminal amino group.

Consequently, the proton bound to the coordinated water molecule is more acidic than the proton bound to the amino group. The first protonation constant ($\log K_a = 5.40$, Table S2) is similar to those describing formation of the monohydroxide species in both the Ga(III)-Dpaa and Ga(III)-Dpaa.ga systems and should be ascribed to the formation of the hydroxide species as well. Thus, the [Ga(Dpaa.dab)] complex is zwitterionic, with a hydroxide anion bound to the Ga(III) and with a protonated amine group. Dissociation constant of the amino group in the complex cannot be determined as it would dissociate at very high pH where the complex is fully decomposed to $[\text{Ga}(\text{OH})_4]^-$. To compare the stability constants, it is more suitable to consider equilibrium between Ga(III) ion and monoprotinated ligand molecule ($\log K_{\text{GaHL}} 16.13$, Table 4) where influence of the above processes is not considered. The value is lower and in line with those for the other systems if the presence of a positive charge, due to a protonated amino group in the ligand molecule, is taken into account. This is reflected in the pM values which are 8.91, 6.34 and 8.21 (pH = 7.4, $[\text{Ga}] = 10^{-6} \text{ M}$, $[\text{L}] = 10^{-5} \text{ M}$) for [Ga(Dpaa)], [Ga(Dpaa.dab)] and [Ga(Dpaa.ga)], respectively. When comparing the formation constant of [Ga(Dpaa)] of 18.53 with that of [Ga(DOTA)] and [Ga(NOTA)] ($\log K_{\text{GaL}} = 26.05$ and 29.60, respectively)^{45, 46} the thermodynamic stability is lower, but still it may be sufficient for the application due to the short half-life of ^{68}Ga .

The stability constants obtained for [Cu(Dpaa)] and [Zn(Dpaa)] complexes are significantly lower than that of the Ga(III) complex (Tables S2 and S3). This may be rationalized due to the low flexibility of the ligand preventing the complex from fulfilling the ideal coordination geometry of these two ligands and due to the high charge density of Ga(III) compared to Cu(II) and Zn(II). The ligands are highly charged with hard oxygen donor atoms and interaction of the ligands with Ga(III) is highly electrostatic in its nature and, therefore, thermodynamic stability of the Ga(III) complexes is increased compared to Cu(II) and Zn(II) complexes. This preference for Ga(III)

complexation is encouraging for biomedical imaging using [^{68}Ga][Ga(Dpaa)] as Cu(II) and Zn(II) are two of the most abundant transition metal ions in vivo.⁴⁷

Whilst the Cu(II) and Zn(II) complexes of H₃Dpaa.dab and H₄Dpaa.ga are less thermodynamically stable than the Ga(III) complexes, the resulting complexes are more stable than those seen with H₃Dpaa. This suggests that the additional coordinating arms may be involved in the complexation of these two metals.

Radiolabelling

The radiochemical yield (RCY) of H₃Dpaa complexing ^{68}Ga was found to have a distinct pH dependence (Figure 4); in acidic aqueous solution the radiochemical yield achieved by 100 μM H₃Dpaa was very high up to pH 4, with a radiochemical yield >95% achieved in 15 minutes at ambient temperature. Above pH 5 the radiochemical yield at ambient temperature fell to approximately 30% after a reaction time of 15 minutes. This is likely due to the formation of gallium hydroxide species with slower complexation kinetics above pH 4.^{6, 13} However, in the presence of 0.1 M phosphate buffer the high RCY was maintained up to pH 7.5, with a 92% yield being achieved in 15 minutes at ambient temperature. Under these conditions ([L] = 100 μM , pH = 7.5, T = 25 °C, I = 0.1 M phosphate buffer, t = 15 minutes), macrocyclic chelators DOTA (0% RCY) and NOTA (48% RCY) performed poorly, but acyclic chelates EDTA (95% RCY) and THP (95% RCY) performed comparably to H₃Dpaa (Table S4). Above pH 8 the RCY of H₃Dpaa fell even in buffered solutions, likely due to the formation of $[\text{Ga}(\text{OH})_4]^-$ as indicated by the potentiometric results (Figure 3). When heated to 37 °C the radiochemical yield achieved at pH 7.5 by 100 μM H₃Dpaa in 15 minutes increased to 95%.

This difference between buffered and aqueous solutions may be explained by a weak gallium-phosphate complex being formed. This may act as a “pre-coordination” complex, preventing the rapid formation of gallium hydroxide species that would result in slower complexation due to the kinetically inert gallium-hydroxide bonds.¹⁹

The pH of the radiolabelling reaction also has a significant effect on the concentration of ligand required for efficient radiolabelling (Figure 5). When radiolabelling at pH 4, efficient complexation is achieved at ligand concentrations as low as 500 nM, with radiochemical yields >90% achieved in 15 minutes at ambient temperature. However, the radiochemical yield sharply decreases below this concentration with no radiolabelling seen when $[H_3Dpaa] = 100 \text{ nM}$. In contrast, at pH 7.4 the radiochemical yield after 15 minutes at ambient temperature is maintained above 90% at 50 μM , however drops below 90% at ligand concentrations of 10 μM .

The ability to rapidly complex ^{68}Ga at neutral pH has the potential to simplify the production of ^{68}Ga labelled radiopharmaceuticals by reducing the post-reaction conditioning required. To develop this further, the complexation of ^{68}Ga by 100 μM H_3Dpaa in saline and phosphate buffered saline (PBS) was assessed. High radio-chemical yields of 99% and 95% respectively were achieved with mild heating (37.7 °C) after 5 minutes. Furthermore, the pH of the PBS solution remained at pH 7.4 after complexation, although the pH of the saline solution was lower (pH 5.5) after addition of the ligand.

The bifunctional chelates $H_3Dpaa.dab$ and $H_4Dpaa.ga$ achieved 99% RCYs after 5 minutes at pH 4 and ambient temperature, and the RCY remained as high as 84% and 94% respectively at pH 7.4 in PBS after 5 minutes at 37 °C (Table 5, Figure S9). Specific activities of 20.0 GBq μmol^{-1} (541 mCi μmol^{-1}) and 28.9 GBq μmol^{-1} (781 mCi μmol^{-1}) were achieved with $H_3Dpaa.dab$ and

H₃Dpaa.ga respectively (Figure S12 and S13) after radiolabelling at pH 4 (T = 25 °C, t = 5 minutes, I = 0.1 M acetate buffer), however H₃Dpaa achieved a specific activity of only 3.9 GBq μmol⁻¹ (105 mCi μmol⁻¹)(Figure S11).

The stability of the radiolabelled complexes formed were assessed against biological competitors, *apo*-transferrin and foetal bovine serum (FBS). Some stability to the iron transport protein *apo*-transferrin was seen, 92% of ⁶⁸Ga activity was associated with the [⁶⁸Ga][Ga(Dpaa)] complex after 2 hours of incubation (Figure S14). In FBS complete decomplexation of the ⁶⁸Ga was seen within 30 minutes for all chelate derivatives (Figure S15). This suggests that having the vacant coordination site filled by H₂O (Figure 2), allows for ⁶⁸Ga to be more readily taken up by competitor proteins found in the serum and therefore H₃Dpaa is not the ideal system for ⁶⁸Ga application *in vivo*.

Conclusions

We describe a ligand system based on amino acids allowing for synthesis of bifunctional chelators. This family of ligands are able to complex ⁶⁸Ga under physiological conditions (5 minutes, pH 7.4 and T = 37.7 °C) at 100 μM. The H₃Dpaa family of ligands are also able to complex ⁶⁸Ga efficiently across a wide pH range. The ligands presented here are more suited to the complexation of small, hard cations like Ga(III) than they are to softer Zn(II) and Cu(II) cations, as indicated by their higher association constants. Studies with biological competitors, FBS and *apo*-transferrin suggest that these chelates are not suited for *in vivo* application with ⁶⁸Ga. However the chelator's preference for Ga(III) and the high radiochemical yield achievable under physiological pH and temperature provides the groundwork to support future studies into acyclic chelators for ⁶⁸Ga.

Experimental Section

NMR spectra were recorded on a JEOL ECP 400 MHz / JEOL Lambda 400 MHz spectrometer using the residual protic solvent signal as an internal reference. ESI Mass spectra were recorded on Advion MS SOP electrospray ionisation spectrometer. pH measurements were carried out using a Jenway model 3520 pH/mV/Temperature meter with a three point calibration. All commercially available starting materials were used without further purification. Ethyl 6-(chloromethyl)picolinate was synthesised from 2,6-dipicolinic acid according to literature methods.^{49, 50} H₃Dpaa and H₃Dpaa.dab were synthesised according to literature methods.^{32, 33}

Synthesis of Et₄Dpaa.ga

To a suspension of l-glutamic acid diethyl ester hydrochloride (1.82 g, 7.6 mmol), potassium carbonate (4.00 g, 28.9 mmol) and potassium iodide (2.64 g, 15.9 mmol) in anhydrous acetonitrile (10 mL) was added ethyl 6-(chloromethyl)picolinate hydrochloride (3.75 g, 15.9 mmol). The mixture was heated to 60 °C for 12 hours. The reaction was quenched with water (50 mL) and extracted with dichloromethane (3 x 100 mL). The combined organic layers were dried with magnesium sulfate and concentrated under reduced pressure. The dark orange oil was purified by column chromatography (silica, 50 mm x 150 mm, Hexane/Ethyl Acetate 20-50%) to yield an orange oil (2.91 g, 5.5 mmol, 72%)

¹H NMR (400 MHz, CDCl₃, 298 K): 7.95 (dd, 2 H, *J* = 6, 2.5 Hz), 7.76 (m, 4H, *py*), 4.46 (q, 4 H, ³*J*_{HH} = 7.1 Hz), 4.22 (qd, 2 H, ³*J*_{HH} = 7.1 Hz, *J* = 1.8 Hz), 4.16 (d, 2 H, ²*J*_{HH} = 15.5 Hz), 4.10 (d, 2 H, ²*J*_{HH} = 15.5 Hz), 4.01 (qt, 2 H, ³*J*_{HH} = 7.1 Hz, *J* = 3.7 Hz), 3.45 (dd, 1 H, *J* = 9.2, 6.1 Hz), 2.50 (m, 2 H), 2.13 (tq, 1 H, ²*J*_{HH} = 14.1 Hz, ³*J*_{HH} = 7.5 Hz), 2.02 (dq, 1 H, ²*J*_{HH} = 14 Hz, ³*J*_{HH} = 7.5 Hz, *J* = 1.6 Hz), 1.44 (t, 6 H, ³*J*_{HH} = 7.1 Hz), 1.33 (t, 3 H, ³*J*_{HH} = 7.1 Hz), 1.18 (t, 3 H, ³*J*_{HH} = 7.1

Hz) ^{13}C NMR (100 MHz, CDCl_3 , 298 K): 173.04, 172.36, 165.26, 160.23, 147.76, 137.21, 125.93, 123.35, 62.33, 61.73, 60.65, 60.25, 57.08, 30.66, 24.79, 14.38, 14.25, 14.08.

Synthesis of $\text{H}_4\text{Dpaa.ga}$

To $\text{Et}_4\text{Dpaa.ga}$ (887 mg, 1.72 mmol) was added 6 M HCl (14 mL). The solution was heated to reflux for 16 hours and then allowed to cool to room temperature. The solvent was removed to yield a yellow oil. Acetone (10 mL) was added to yield an off-white precipitate (617 mg, 1.26 mmol, 73 %).

^1H NMR (400 MHz, D_2O (pD = 7.1), 298 K), δ : 7.72-7.55 (m, 4 H), 7.42-7.32 (m, 2 H), 4.47-4.33 (m, 4 H), 3.77-3.63 (m, 1 H), 2.43-2.27 (m, 2H), 2.27-2.06 (m, 2 H). ^{13}C NMR (100 MHz, D_2O (pD = 7.1), 298 K), δ : 181.70, 176.22, 171.57, 153.47, 151.81, 138.88, 126.17, 123.11, 69.52, 57.14, 34.51, 25.67 MS (ESI), m/z : 418.04 $[\text{M}+\text{H}]^+$. Elemental Analysis (C/H/N), %: Expected for $\text{H}_4\text{Dpaa.ga} \cdot 2\text{HCl}$ ($\text{C}_{19}\text{H}_{21}\text{Cl}_2\text{N}_3\text{O}_8$): 46.55/4.32/8.57 Found: 46.22/4.40/7.99

H_3Dpaa

Et_3Dpaa (38 mg, 0.089 mmol) in 6M HCl (6 mL) was heated to reflux for 16 h. The sample was concentrated, ethanol added, and the precipitate collected and washed with diethyl ether to yield a white solid (36.5 mg, 0.089 mmol, 100%)

^1H NMR (400 MHz, D_2O (pD = 8.8), 298 K), δ : 7.72-7.62 (m, 4 H), 7.38 (br d, 2 H, $^3J_{\text{HH}} = 7.8$ Hz), 3.92(br s, 4 H), 3.27 (br s, 2 H). ^{13}C NMR (100 MHz, D_2O (pD = 8.8), 298 K), δ : 172.96, 152.71, 138.14, 125.87, 122.35, 60.07, 59.22 MS(ESI), $m/z = 346.4$ $[\text{M}+\text{H}]^+$. Elemental Analysis

(C/H/N), %: Expected for $\text{H}_3\text{Dpaa}.1.3(\text{HCl})0.25(\text{diethyl ether})$ ($\text{C}_{17}\text{H}_{19.05}\text{Cl}_{1.3}\text{N}_3\text{O}_{6.25}$): 49.62/4.67/10.21 Found: 49.63/4.40/9.94

$\text{H}_3\text{Dpaa.dab}$

$\text{Et}_2\text{MeDpaa.dab}(\text{Boc})$ (676.4 mg, 1.21 mmol) was dissolved in 6 M HCl (20 mL) and heated to reflux overnight. The solvent was removed under reduced pressure to yield a yellow oil. Addition of acetone resulted in precipitation of a solid. Isolation of this precipitate yielded a yellow solid (446.3 mg, 0.84 mmol, 70%).

^1H NMR (400 MHz, D_2O (pD = 1.6), 298 K), δ : 8.09 (t, 2 H, $^3J_{\text{HH}} = 7.8$ Hz), 7.96 (d, 2 H, $^3J_{\text{HH}} = 7.8$ Hz), 7.71 (d, 2 H, $^3J_{\text{HH}} = 7.8$ Hz), 4.41 (s, 4 H), 4.00 (t, 1 H, $^3J_{\text{HH}} = 7.3$ Hz), 3.37-3.18 (m, 2 H), 2.40-2.23 (m, 2 H). ^{13}C NMR (100 MHz, D_2O (pD = 1.6), 298 K), δ : 174.50, 164.62, 154.61, 145.26, 143.74, 128.24, 124.92, 64.99, 55.53, 37.66, 26.10. MS (ESI) m/z: 389.4 $[\text{M}+\text{H}]^+$.
Elemental Analysis (C/H/N), %: Expected for $\text{H}_3\text{Dpaa.dab}(\text{HCl})_3(\text{Acetone})_{0.55}$ ($\text{C}_{19.65}\text{H}_{28.3}\text{Cl}_3\text{N}_4\text{O}_{7.55}$): 43.09/5.21/10.23 Found 42.85/5.15/9.93

Synthesis of $[\text{Ga}(\text{Dpaa.ga})]$

To $\text{H}_4\text{Dpaa.ga}$ (25 mg, 0.062 mmol) in a solution of methanol (1 mL) and water (1 mL) was added GaCl_3 (10.9 mg, 0.062 mmol) in water (1.2 mL). The solution was heated to 70 °C for 16 hours and allowed to cool. The precipitate was collected by centrifugation (4000 rpm, 3 minutes) to give a white solid (14.6 mg, 0.026 mmol, 42%).

^1H NMR (400 MHz, D_2O (pD = 6.0), 298 K) δ : 8.30-8.11 (m, 4 H), 7.81-7.73 (m, 2 H), 4.66 (br d, 2 H, $^2J_{\text{HH}} = 17$ Hz), 4.33 (br d, 2 H, $^2J_{\text{HH}} = 17$ Hz), 3.05-2.97 (m, 1 H), 2.44-2.33 (m, 1 H), 2.26-2.15 (m, 1 H), 2.06-1.88 (m, 2 H). ^{13}C NMR (100 MHz, D_2O (pD = 6.0), 298 K) δ : 180.94, 178.13,

168.10, 152.32, 151.03, 144.69, 144.45, 142.83, 142.76, 127.57, 126.38, 123.11, 123.06, 62.08, 58.28, 53.07, 34.80, 22.33. MS (ESI), m/z : 483.94 [$^{69}\text{GaM}+\text{H}$] $^{+}$, 485.97 [$^{71}\text{GaM}+\text{H}$] $^{+}$. Elemental Analysis (C/H/N), %: Expected for $\text{GaDpaa.g}(\text{COOH})\cdot 3.5\text{H}_2\text{O}\cdot 0.5\text{MeOH}$ ($\text{C}_{19.5}\text{H}_{25}\text{GaN}_3\text{O}_{12}$): 41.59/4.47/7.46 Found: 41.56/4.68/7.42

Synthesis of [Ga(Dpaa)]

To H_3Dpaa (76 mg, 0.22 mmol) in water (5 mL) was added GaCl_3 (38.8 mg, 0.22 mmol) in water (3.8 mL). The pH was adjusted to 4.5 with sodium hydroxide. The solution was heated to reflux for 3 days. After cooling, the solution was filtered to give a white solid (76 mg, 0.14 mmol, 64%).

^1H NMR (400 MHz, D_2O (pD = 8.8), 298 K) δ : 8.21 (t, 2 H, $^3J_{\text{HH}} = 7.3$ Hz), 8.14 (d, 2 H, $^3J_{\text{HH}} = 7.3$ Hz), 7.75 (d, 2 H, $^3J_{\text{HH}} = 7.3$ Hz), 4.62 (dd, 2 H, $^2J_{\text{HH}} = 16.0$ Hz, $^4J_{\text{HH}} = 2.75$ Hz), 4.48 (br d, 2 H, $^2J_{\text{HH}} = 16.0$ Hz), 3.39 (d, 2 H, $^4J_{\text{HH}} = 2.3$ Hz). ^{13}C NMR (100 MHz, D_2O (pD = 8.8), 298 K) δ : 176.86, 168.40, 151.26, 144.57, 142.35, 126.76, 122.99, 60.60, 59.89. MS (ESI), m/z : 411.95 [$^{69}\text{GaM}+\text{H}$] $^{+}$, 413.89 [$^{71}\text{GaM}+\text{H}$] $^{+}$. Elemental Analysis (C/H/N), %: Expected for $\text{GaDpaa}\cdot\text{H}_2\text{O}\cdot 3\text{HCl}$ ($\text{C}_{16}\text{H}_{17}\text{Cl}_3\text{GaN}_3\text{O}_7$): 35.63/3.18/7.79 Found: 35.85/3.09/7.59

Synthesis of [Ga(Dpaa.dab)]

To $\text{H}_3\text{Dpaa.dab}$ (25 mg, 0.064 mmol) in methanol (5 mL) was added GaCl_3 (11.3 mg, 0.064 mmol) in water (1.2 mL). This solution was heated to 70 °C for 1 hour and allowed to cool. The precipitate was collected by centrifugation (4000 rpm, 3 minutes) to give a white solid (17 mg, 0.039 mmol, 60%)

^1H NMR (400 MHz, D_2O (pD = 1.1), 298 K) δ : 8.32-8.24 (m, 2 H), 8.24-8.12 (m, 2 H), 7.88-7.75 (m, 2 H), 4.56-4.33 (m, 3 H), 4.07 (br d, 1 H, $^2J_{\text{HH}} = 17.4$ Hz), 3.18-3.12 (m, 1 H), 3.11-3.02 (m, 2

H), 2.28-2.07 (m, 3 H). ^{13}C NMR (100 MHz, D_2O (pD = 1.1), 298 K) δ : 177.21, 167.18, 167.05, 153.37, 152.71, 145.06, 144.69, 143.97, 128.49, 127.67, 123.77, 123.63, 61.19, 65.00, 51.95, 38.11, 30.30, 24.07. MS (ESI), m/z : 454.43 [$^{69}\text{GaM}+\text{H}$] $^+$, 456.39 [$^{71}\text{GaM}+\text{H}$] $^+$. Elemental Analysis (C/H/N), %: Expected for $\text{GaDpaa.dab}(\text{NH}_2)\cdot\text{H}_2\text{O}\cdot 0.9\text{HCl}$ ($\text{C}_{18}\text{H}_{19.9}\text{Cl}_{0.9}\text{GaN}_4\text{O}_7$): 42.73/3.97/11.07 Found: 43.02/3.63/10.87

Potentiometry

Potentiometry was carried out according to previously published procedures.^{51, 52} Protonation and stability constants were determined in 0.1 M $(\text{NMe}_4)\text{Cl}$ at 25.0 °C with $pK_w = 13.81$. Protonation constants ($[\text{L}] = 0.004$ M) were determined from data obtained in pH range 1.6–12.1 (~40 points per titration and three parallel titrations) with electrode calibrated by acid-base titration in extended pH ranges (1.7–12.2 for each titration set). Complex stability constants ($[\text{L}] = [\text{M}] = 0.004$ M) were determined from data obtained in pH range 1.5–12.1, 50 data points per titration, three parallel titrations).

UV-VIS spectra were recorded on spectrophotometer Specord 50 Plus (Analytik Jena AG). Temperature was maintained by Peltier block. UV-VIS titration of the $\text{Ga(III)}\text{-H}_3\text{Dpaa}$ system ($[\text{L}] = [\text{M}] = 0.0001$ M) was performed at pH range 2.4–6.9 in 0.1 M $(\text{NMe}_4)\text{Cl}$, pH was adjusted with ~0.2 M $(\text{NMe}_4)\text{OH}$ using a glass electrode. UV-VIS titrations of the Cu(II) and Zn(II) systems with $\text{H}_4\text{Dpaa.ga}$ and $\text{H}_3\text{Dpaa.dab}$ ($[\text{L}] = [\text{M}] = 0.00001$ M) were performed at pH range 0.0–2.0 without ionic strength control, pH was calculated from added amount of HCl .

The titration and UV-VIS data were treated simultaneously with OPIUM program package.^{53, 54} Calculated constants are concentration constants defined as $\beta_{hl} = [\text{H}_h\text{L}_l] / [\text{H}]_h \cdot [\text{L}]_l$ or $\beta_{hlm} =$

$[H_h L_l M_m] / [H]^h \cdot [L]^l \cdot [M]^m$ and standard deviations are given directly by the program. pM values were also calculated by OPIUM from determined protonation and stability constants.

The full version of the OPIUM program is available (free of charge) on http://www.natur.cuni.cz/_kyvala/opium.html

Radiolabelling

The IGG100 generator was eluted with 0.6 M aq. HCl (3 mL). This eluate (300-200 MBq) was diluted with H₂O (15 mL) and passed through a Strata-X-C 33 µM Cation Mixed-mode polymeric support. The activity was liberated from the column using 98:2 acetone:0.1 M aq. HCl (1 mL). Aliquots (~30 MBq) of this solution were dried under a stream of inert gas at 90 °C and allowed to cool before use. 1 mL of ligand solution was added to the dried ⁶⁸Ga and shaken. 5 µL aliquots were taken for analysis by TLC and 20 µL aliquots for analysis by HPLC.

TLC analysis was performed on Kieselgel 60 F254 plates (Merck) with an eluate of 0.1 M citric acid in water. HPLC analysis was carried out using an Agilent Zorbax Eclipse XDB-C18 column and a solvent system of water + 0.1% TFA and methanol.

Assessment of stability to apo-transferrin

100 µL of radiolabelling solution containing 100 µM H₃Dpaa in 0.1 M acetate buffer (pH 4.5) after incubation with gallium-68 for 5 minutes was added to 600 µL of 1 mgml⁻¹ transferrin in 0.1 M sodium hydrogen carbonate solution to give a final pH of 7.2. This solution was incubated at 37 °C with aliquots taken at 60 and 120 minutes for HPLC analysis (figure S13).

Assessment of stability in foetal bovine serum

100 μ L of radiolabelling solution containing 100 μ M ligand in PBS (pH 7.4) was added to 1.5 mL of foetal bovine serum and incubated at 37 °C. Aliquots were taken at 30minutes for TLC analysis (figure S14).

Analytical HPLC gradient: Solvent A: Water + 0.1% TFA, Solvent B: Methanol. Flow rate = 1 mL min⁻¹. Column Size: 4.6 x 150 mm with 4.6 x 12.5 mm guard column [Time / mins](A:B). [0-3](95:5). [3-18](95:5 – 5:95). [18-20](5:95). [20-25](5:95 – 95:5). [25-30](95:5)

Semi-preparative HPLC gradient: Solvent A: Water + 0.1% TFA, Solvent B: Methanol. Flow rate = 3 mL min⁻¹. Column Size: 9.4 x 250 mm. [Time / mins](A:B). [0-10](95:5). [10-11](95:5 – 5:95). [11-14](5:95). [14-15](5:95-95:5) [15-20](95:5)

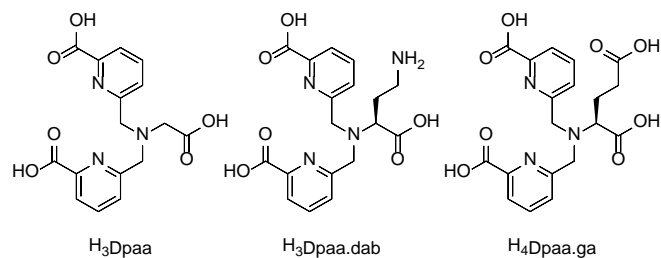
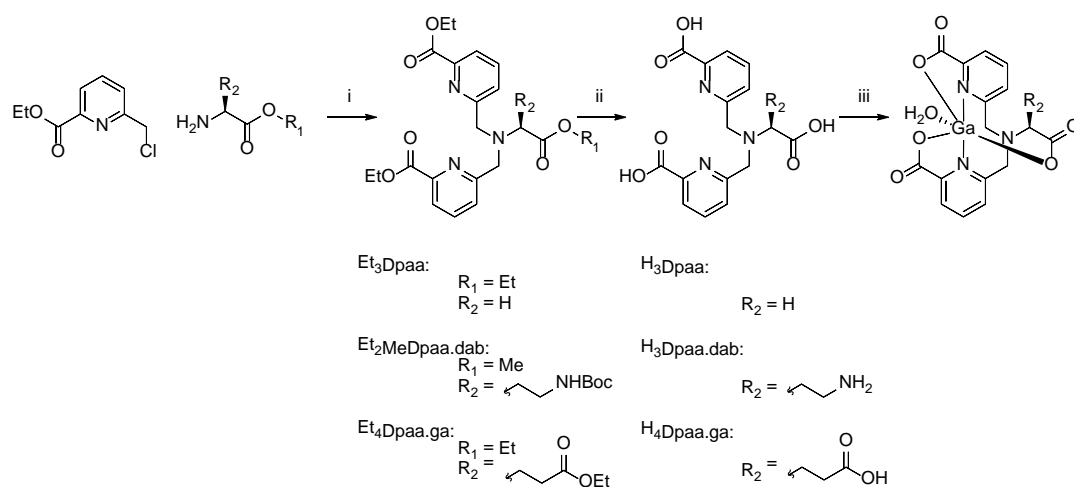


Figure 1. Ligands described in this work



Scheme 1. Synthetic scheme for the synthesis of ligands reported in this paper. i) K_2CO_3 , KI, MeCN, 60 °C, 12 h. ii) 6 M HCl, reflux, 16 h, iii) GaCl_3 , H_2O , pH 4

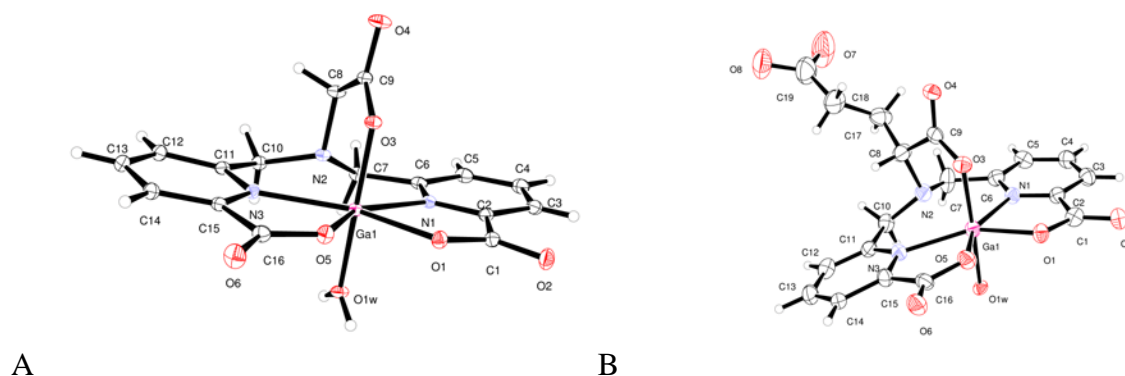


Figure 2. ORTEP representations of molecular structures of A) $[\text{Ga}(\text{H}_2\text{O})(\text{Dpaa})]^\ddagger$ and B) $[\text{Ga}(\text{H}_2\text{O})(\text{Dpaa.ga})]^\S$ obtained by single crystal x-ray crystallography (drawn with 30% certainty, solvent molecules omitted for clarity).

Table 1. Selected crystallographic parameters (Bond lengths) for GaDpaa and GaDpaa.ga

Bond length / Å		
Bond	GaDpaa	GaDpaa.ga
O1-Ga1	2.0441(10)	2.001(6)
N1-Ga1	2.2354(11)	2.191(7)
N2...Ga1	2.4880(11)	2.513(8)
N3-Ga1	2.2017(12)	2.180(7)
O5-Ga1	2.0229(10)	2.034(6)
O3-Ga1	1.9173(10)	1.942(6)
O1W-Ga1	1.9109(10)	1.952(5)

Table 2. Selected crystallographic parameters (Bond angles) for GaDpaa and GaDpaa.ga

Bond Angle / °		
Angle	GaDpaa	GaDpaa.ga
O1-Ga1-N1	73.97(4)	76.1(3)
N1-Ga1-N3	135.16(4)	133.7(3)
N3-Ga1-O5	74.95(4)	75.2(3)
O5-Ga1-O1	75.92(4)	75.5(3)
O3-Ga1-O1	90.08(4)	93.8(3)
O3-Ga1-N1	88.09(4)	86.0(2)
O3-Ga1-N3	91.36(4)	96.4(3)
O3-Ga1-O5	92.23(4)	90.7(2)
O3-Ga1-O1W	175.40(4)	172.8(2)

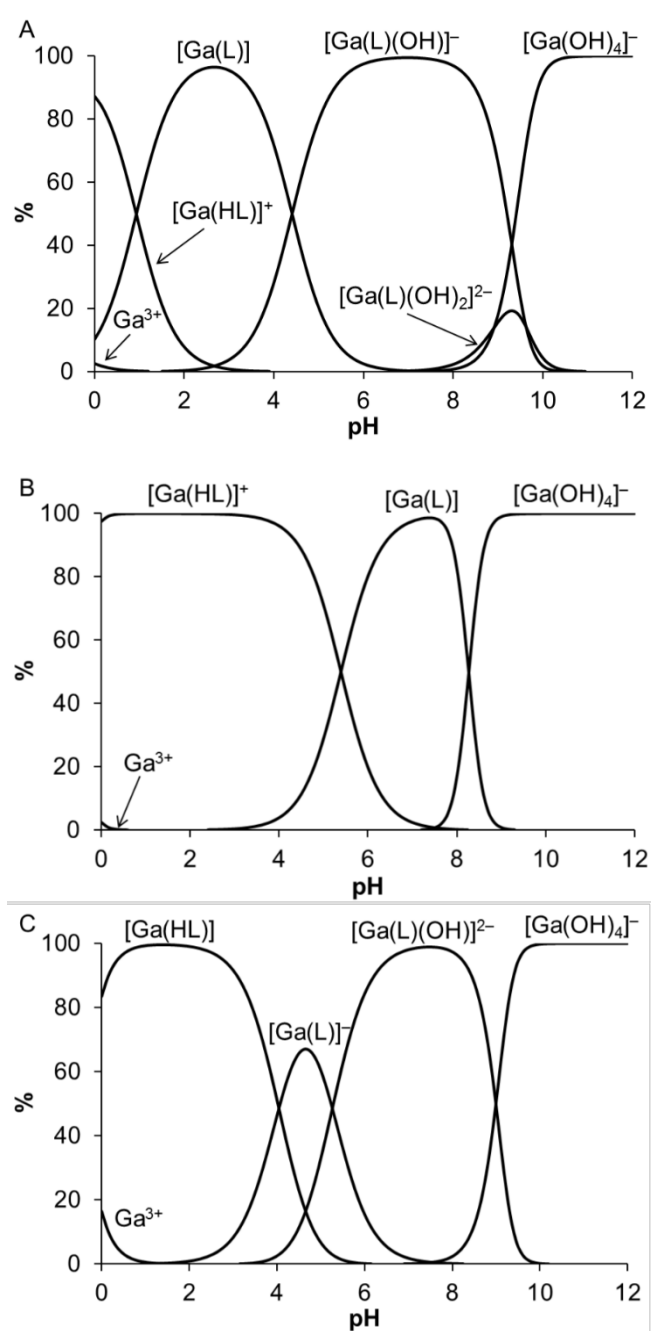


Figure 3. Speciation diagrams for Ga(III) – ligand systems. A) H₃Dpaa, B) H₃Dpaa.dab(NH₂), C) H₄Dpaa.ga ($T = 25\text{ }^\circ\text{C}$, $I = 0.1\text{ M}$ (NMe₄)Cl, $[\text{L}] = [\text{Ga(III)}] = 0.004\text{ M}$).

Table 3. Stepwise protonation constants obtained for ligands by potentiometry^a

	H₃Dpaa	H₃Dpaa.dab	H₄Dpaa.ga
<i>logK</i> ₁	7.38	11.35	7.17
<i>logK</i> ₂	3.73	5.39	4.67
<i>logK</i> ₃	2.82	3.77	3.92
<i>logK</i> ₄	-	2.69	2.75

^[a] ([L] = 0.004 M, *T* = 25 °C, *I* = 0.1 M (NMe₄)Cl)

Table 4. Stability constants (*logK*) obtained for complexes.

Metal Ion	H₃Dpaa	H₃Dpaa.dab	H₄Dpaa.ga
Ga(III)	18.53 ^[a]	22.08 ^[b] 16.13 ^[b,c]	18.36 ^[b]
Cu(II)	10.85 ^[b]	19.1 ^[b,d]	14.52 ^[b,d]
Zn(II)	11.93 ^[b]	15.8 ^[b,d]	13.38 ^[b,d]

^[a] Determined by UV-VIS titration [L] = [M] = 0.1 mM, *T* = 25 °C, pH = 2-7 ^[b]Determined by potentiometric titration ([L] = [M] = 0.004 M, *T* = 25 °C, *I* = 0.1 M (NMe₄)Cl), ^[c]Constant (*logK*_{GaHL}) describing equilibrium Ga(III) + (HL)²⁻ ↔ [Ga(HL)]⁺ where the amine group deprotonation and hydroxido species formation are not considered. ^[d] Determined by UV-VIS titration ([L] = [M] = 0.01 mM, *T* = 25 °C, pH = 0-2)

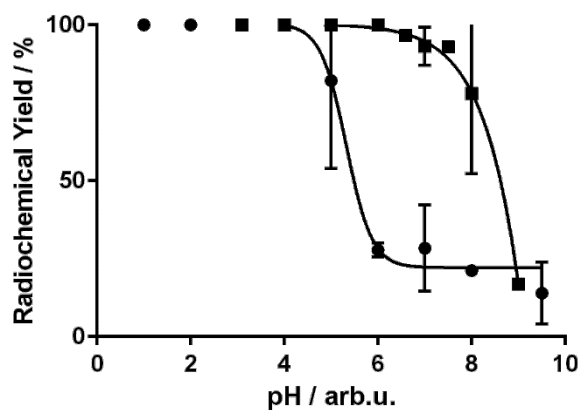


Figure 4. pH titration of radiochemical yield for formation of $[^{68}\text{Ga}][\text{Ga}(\text{Dpaa})]$. Circles, I = unbuffered aqueous solution. Squares, I = 0.1 M buffered solution, ($[\text{H}_3\text{Dpaa}] = 100 \mu\text{M}$, $T = 25^\circ\text{C}$, $t = 15$ minutes)

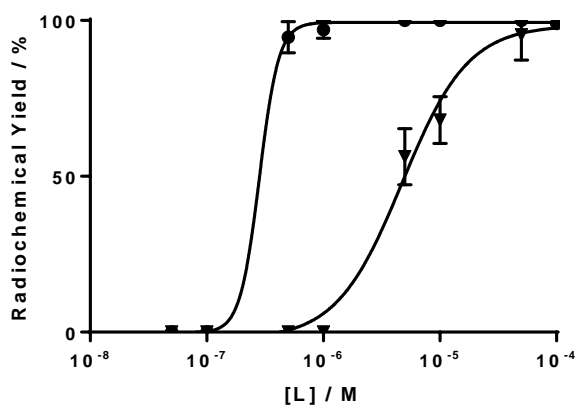


Figure 5. Radiochemical yield for formation of $[^{68}\text{Ga}][\text{Ga}(\text{Dpaa})]$ at varying concentrations. Circles = pH 4.0, I = 0.1 M acetate solution. Triangles = pH 7.4, I = 0.1 M phosphate solution, ($T = 25^\circ\text{C}$, $t = 15$ minutes)

Table 5. Radiochemical yields of labelling reactions^[a]

Ligand	H₃Dpaa	H₃Dpaa.dab	H₄Dpaa.ga
pH 4.0 ^[b]	99%	99%	99%
pH 7.4 ^[c]	95%	84%	94%

^[a] $[\text{L}] = 100 \mu\text{M}$ ligand, $t = 5$ minutes ^[b] $I = 0.1$ M Acetate, $T = 25^\circ\text{C}$, ^[c] $I = \text{PBS}$, $T = 37.7^\circ\text{C}$

Acknowledgements

The authors would like to thank the University of Hull for the PhD studentship and The Royal Society for the research grant RG160156, for a ^{68}Ga generator, which funded this project. The authors would also like to thank Sergei Palmer for his input. We thank the EPSRC UK National Crystallography Service at the University of Southampton for the collection of the crystallographic data.⁵⁵

Supporting Information. CCDC-1530703 ([Ga(Dpaa.ga)]), CCDC-1530704 ($\text{H}_4\text{Dpaa.ga}$) & CCDC-1549314 ([Ga(Dpaa)]) contain the supplementary crystallographic data for this paper. These data are provided free of charge by The Cambridge Crystallographic Data Centre.

Notes

$^{\dagger\dagger}\text{H}_4\text{Dpaa.ga}$ crystal structure data: refined formula $\text{C}_{19}\text{H}_{19}\text{N}_3\text{O}_8$; $M_r = 417.37$; crystal dimensions $0.275 \times 0.130 \times 0.056 \text{ mm}^3$; Monoclinic; $P2_1/n$; $a = 7.0852(6) \text{ \AA}$, $b = 32.290(4) \text{ \AA}$, $c = 7.6786(6) \text{ \AA}$, $\beta = 94.108(7)^\circ$, $V = 1752.2(3) \text{ \AA}^3$; $Z = 4$; $\rho_{\text{calcd}} = 1.582 \text{ g cm}^{-3}$; $\mu = 0.125 \text{ mm}^{-1}$; Mo $K\alpha$ radiation $\lambda = 0.7173 \text{ \AA}$; $T = 150 \text{ K}$; $2\theta_{\text{max}} = 51.10^\circ$; no. of reflections measured (independent) = 9845 (3229); $R_{\text{int}} = 0.0571$; $R = 0.0401$; $wR2 = 0.0612$; $\rho_{\text{max/min}} = 0.172 / -0.197 \text{ e \AA}^{-3}$; data collected using a Stoe IPDS2 diffractometer; structure solved by routine dual space methods and refined against all observed F^2 values.

$^{\ddagger}\text{GaDpaa}$ crystal structure data: refined formula $\text{C}_{16}\text{H}_{20}\text{Ga}_1\text{N}_3\text{O}_{10}$; $M_r = 484.07$; crystal dimensions $0.040 \times 0.005 \times 0.005 \text{ mm}^3$; Triclinic; $P-1$; $a = 7.06810(10) \text{ \AA}$, $b = 8.21920(10) \text{ \AA}$, $c = 15.9952(2) \text{ \AA}$, $\alpha = 93.6180(10)^\circ$, $\beta = 93.7920(10)^\circ$, $\gamma = 91.9130(10)^\circ$, $V = 924.69(2) \text{ \AA}^3$; $Z = 1$; $\rho_{\text{calcd}} = 1.739 \text{ g cm}^{-3}$; $\mu = 1.425 \text{ mm}^{-1}$; synchrotron radiation $\lambda = 0.6889 \text{ \AA}$; $T = 100 \text{ K}$; $2\theta_{\text{max}} = 72.358^\circ$; no. of reflections measured (independent) = 20701 (8614); $R_{\text{int}} = 0.057$; $R = 0.0425$; $wR2 = 0.1062$;

$\rho_{max/min} = 1.606 / -0.543 \text{ e } \text{\AA}^{-3}$; data collected at Diamond synchrotron UK, station I19; structure solved by routine dual space methods and refined against all observed F^2 values.

$^{\text{§}}\text{GaDpaa.ga}$ crystal structure data: refined formula $\text{C}_{19}\text{H}_{24}\text{GaN}_3\text{O}_{12.5}$; $M_r = 564.12$; crystal dimensions $0.060 \times 0.005 \times 0.005 \text{ mm}^3$; Orthorhombic; $Pccn$; $a = 20.7850(12) \text{ \AA}$, $b = 30.2224(18) \text{ \AA}$, $c = 7.2085(6) \text{ \AA}$, $V = 4528.2(5) \text{ \AA}^3$; $Z = 8$; $\rho_{\text{calcd}} = 1.646 \text{ g cm}^{-3}$; $\mu = 1.186 \text{ mm}^{-1}$; synchrotron radiation $\lambda = 0.6889 \text{ \AA}$; $T = 100 \text{ K}$; $2\theta_{\text{max}} = 49.67^\circ$; no. of reflections measured (independent) = 12211 (4251); $R_{\text{int}} = 0.2109$; $R = 0.0999$; $wR = 0.2359$; $\rho_{max/min} = 2.429 / -1.265 \text{ e } \text{\AA}^{-3}$; disordered water was modelled using the SQUEEZE routine; data collected at Diamond synchrotron UK, station I19; the crystal suffers from radiation damage but structure solution and refinement were routine; structure solved by routine dual space methods and refined against all observed F^2 values.

References

1. S. S. Gambhir, *Nature Reviews Cancer*, 2002, **2**, 683.
2. S. M. Ametamey, M. Honer and P. A. Schubiger, *Chemical Reviews*, 2008, **108**, 1501-1516.
3. P. W. Miller, N. J. Long, R. Vilar and A. D. Gee, *Angew. Chem. Int. Ed.*, 2008, **47**, 8998-9033.
4. T. W. Price, J. Greenman and G. J. Stasiuk, *Dalton Transactions*, 2016, **45**, 15702-15724.
5. D. Brasse and A. Nonat, *Dalton Transactions*, 2015, **44**, 4845-4858.
6. M. Fani, J. P. André and H. R. Maecke, *Contrast Media Mol. Imaging*, 2008, **3**, 53-63.
7. E. W. Price and C. Orvig, *Chem. Soc. Rev.*, 2014, **43**, 260-290.
8. F. Rösch, *Applied Radiation and Isotopes*, 2013, **76**, 24-30.
9. I. Velikyan, *Journal of Labelled Compounds and Radiopharmaceuticals*, 2015, **58**, 99-121.
10. M. D. Bartholomä, A. S. Louie, J. F. Valliant and J. Zubieta, *Chemical Reviews*, 2010, **110**, 2903-2920.
11. X. Sun, Y. Li, T. Liu, Z. Li, X. Zhang and X. Chen, *Advanced Drug Delivery Reviews*, 2016, DOI: 10.1016/j.addr.2016.06.007, In Press.

12. B. P. Burke, G. S. Clemente and S. J. Archibald, *J. Label. Compd. Radiopharm.*, 2014, **57**, 239-243.
13. M. D. Bartholomä, *Inorg. Chim. Acta*, 2012, **389**, 36-51.
14. P. Spang, C. Herrmann and F. Roesch, *Semin. Nucl. Med.*, 2016, **46**, 373-394.
15. L. Wei, Y. Miao, F. Gallazzi, T. P. Quinn, M. J. Welch, A. L. Vāvere and J. S. Lewis, *Nucl. Med. Biol.*, 2007, **34**, 945-953.
16. I. Velikyan, H. Maecke and B. Langstrom, *Bioconjugate Chem.*, 2008, **19**, 569-573.
17. G. J. Stasiuk and N. J. Long, *Chem. Commun.*, 2013, **49**, 2732-2746.
18. G. Kramer-Marek, N. Shenoy, J. Seidel, G. L. Griffiths, P. Choyke and J. Capala, *Eur J Nucl Med Mol Imaging*, 2011, **38**, 1967-1976.
19. I. Velikyan, *Theranostics*, 2014, **4**, 47-80.
20. B. M. Zeglis, J. L. Houghton, M. J. Evans, N. Viola-Villegas and J. S. Lewis, *Inorganic Chemistry*, 2014, **53**, 1880-1899.
21. D. J. Berry, Y. M. Ma, J. R. Ballinger, R. Tavare, A. Koers, K. Sunassee, T. Zhou, S. Nawaz, G. E. D. Mullen, R. C. Hider and P. J. Blower, *Chem. Commun.*, 2011, **47**, 7068-7070.
22. J. Seemann, B. P. Waldron, F. Roesch and D. Parker, *ChemMedChem*, 2015, **10**, 1019-1026.
23. J. Seemann, B. Waldron, D. Parker and F. Roesch, *EJNMMI Radiopharmacy and Chemistry*, 2016, **1**, 1-12.
24. M. T. Ma, C. Cullinane, C. Imberti, J. Bagaña Torres, S. Y. A. Terry, P. Roselt, R. J. Hicks and P. J. Blower, *Bioconjugate Chemistry*, 2016, **27**, 309-318.
25. M. T. Ma, C. Cullinane, K. Waldeck, P. Roselt, R. J. Hicks and P. J. Blower, *EJNMMI Research*, 2015, **5**, 1-11.
26. B. Baur, E. Andreolli, E. Al-Momani, N. Malik, H.-J. Machulla, S. N. Reske and C. Solbach, *J Radioanal Nucl Chem*, 2014, **299**, 1715-1721.
27. B. Baur, C. Solbach, E. Andreolli, G. Winter, H.-J. Machulla and S. Reske, *Pharmaceuticals*, 2014, **7**, 517.
28. C. Zhai, D. Summer, C. Rangger, H. Haas, R. Haubner and C. Decristoforo, *Journal of Labelled Compounds and Radiopharmaceuticals*, 2015, **58**, 209-214.
29. S. Ray Banerjee, Z. Chen, M. Pullambhatla, A. Lisok, J. Chen, R. C. Mease and M. G. Pomper, *Bioconjugate Chemistry*, 2016, **27**, 1447-1455.
30. E. Boros, C. L. Ferreira, J. F. Cawthray, E. W. Price, B. O. Patrick, D. W. Wester, M. J. Adam and C. Orvig, *J. Am. Chem. Soc.*, 2010, **132**, 15726-15733.
31. A. M. Nonat, C. Gateau, P. H. Fries, L. Helm and M. Mazzanti, *Eur. J. Inorg. Chem.*, 2012, **2012**, 2049-2061.
32. A. Nonat, P. H. Fries, J. Pécaut and M. Mazzanti, *Chemistry – A European Journal*, 2007, **13**, 8489-8506.
33. G. J. Stasiuk, S. Tamang, D. Imbert, C. Gateau, P. Reiss, P. Fries and M. Mazzanti, *Dalton Transactions*, 2013, **42**, 8197-8200.
34. A. Forgacs, R. Pujales-Paradela, M. Regueiro-Figueroa, L. Valencia, D. Esteban-Gomez, M. Botta and C. Platas-Iglesias, *Dalton Transactions*, 2017, **46**, 1546-1558.
35. D. M. Weekes, C. F. Ramogida, M. d. G. Jaraquemada-Peláez, B. O. Patrick, C. Apte, T. I. Kostelnik, J. F. Cawthray, L. Murphy and C. Orvig, *Inorganic Chemistry*, 2016, **55**, 12544-12558.
36. K. G. Kadiyala, T. Tyagi, D. Kakkar, N. Chadha, K. Chuttani, B. G. Roy, M. Thirumal, A. K. Mishra and A. Datta, *RSC Advances*, 2015, **5**, 33963-33973.

37. E. Boros, Y.-H. S. Lin, C. L. Ferreira, B. O. Patrick, U. O. Hafeli, M. J. Adam and C. Orvig, *Dalton Transactions*, 2011, **40**, 6253-6259.
38. A. Forgács, M. Regueiro-Figueroa, J. L. Barriada, D. Esteban-Gómez, A. de Blas, T. Rodríguez-Blas, M. Botta and C. Platas-Iglesias, *Inorganic Chemistry*, 2015, **54**, 9576-9587.
39. B. Gery, M. Gennari, E. Goure, J. Pecaut, A. Blackman, D. A. Pantazis, F. Neese, F. Molton, J. Fortage, C. Duboc and M.-N. Collomb, *Dalton Transactions*, 2015, **44**, 12757-12770.
40. Y. Bretonnière, M. Mazzanti, J. Pécaut, F. A. Dunand and A. E. Merbach, *Inorganic Chemistry*, 2001, **40**, 6737-6745.
41. N. Chatterton, Y. Bretonnière, J. Pécaut and M. Mazzanti, *Angewandte Chemie International Edition*, 2005, **44**, 7595-7598.
42. A. Pellissier, Y. Bretonnière, N. Chatterton, J. Pécaut, P. Delangle and M. Mazzanti, *Inorganic Chemistry*, 2007, **46**, 3714-3725.
43. S. L. Madsen, M. J. Welch, R. J. Motekaitis and A. E. Martell, *International Journal of Radiation Applications and Instrumentation. Part B. Nuclear Medicine and Biology*, 1992, **19**, 431-444.
44. A. Schmidtke, T. Lämpchen, C. Weinmann, L. Bier-Schorr, M. Keller, Y. Kiefer, J. P. Holland and M. D. Bartholomä, *Inorganic Chemistry*, 2017, **56**, 9097-9110.
45. V. Kubíček, J. Havlíčková, J. Kotek, G. Tircsó, P. Hermann, É. Tóth and I. Lukeš, *Inorg. Chem.*, 2010, **49**, 10960-10969.
46. J. Simecek, M. Schulz, J. Notni, J. Plutnar, V. Kubicek, J. Havlickova and P. Hermann, *Inorg. Chem.*, 2012, **51**, 577-590.
47. P. J. Blower, J. S. Lewis and J. Zweit, *Nucl. Med. Biol.*, 1996, **23**, 957-980.
48. P. K. Glasoe and F. A. Long, *The Journal of Physical Chemistry*, 1960, **64**, 188-190.
49. R. Fornasier, D. Milani, P. Scrimin and U. Tonellato, *Journal of the Chemical Society, Perkin Transactions 2*, 1986, DOI: 10.1039/P29860000233, 233-237.
50. M. Mato-Iglesias, A. Roca-Sabio, Z. Pálkás, D. Esteban-Gómez, C. Platas-Iglesias, É. Tóth, A. de Blas and T. Rodríguez-Blas, *Inorganic Chemistry*, 2008, **47**, 7840-7851.
51. P. Táborický, P. Lubal, J. Havel, J. Kotek, P. Hermann and I. Lukeš, *Collect. Czech. Chem. Commun.*, 2005, **70**, 1909-1942.
52. M. Försterová, I. Svobodová, P. Lubal, P. Táborický, J. Kotek, P. Hermann and I. Lukeš, *Dalton Transactions*, 2007, DOI: 10.1039/B613404A, 535-549.
53. M. Kývala and I. Lukeš, presented in part at the International Conference Chemometrics '95, Pardubice, Czech Republic, 1995.
54. M. Kývala, P. Lubal and I. Lukeš, presented in part at the Spanish-Italian and Mediterranean Congress on Thermodynamics of Metal Complexes (SIMEC 98), Girona, Spain, 1998.
55. S. J. Coles and P. A. Gale, *Chemical Science*, 2012, **3**, 683-689.